

Reconstruction transitions during molecular-beam epitaxy on GaAs(111)*B* vicinal surfaces studied by scanning electron microscopy

Hong-Wen Ren* and Tatau Nishinaga

Graduate School of Engineering, The University of Tokyo, 7-3-1 Hongo, Bunkyo-ku, Tokyo 113, Japan

(Received 9 July 1996)

Real-time imaging of reconstruction transitions during molecular-beam epitaxy on a GaAs surface has been performed by scanning electron microscopy in the secondary-electron mode, and reconstruction-transition-associated step bunching as well as debunching behaviors were investigated. On the GaAs(111)*B* surface inclined 1° toward the $[\bar{1}1\bar{2}]$ direction, uniform motion of atomic steps was observed at 620°C with a growth rate of 0.1 ML/s under $\sqrt{19}\times\sqrt{19}$ reconstruction. When the growth temperature was raised to 625°C , 1×1 high-temperature reconstruction $[(1\times 1)_{\text{HT}}]$ was found to appear from the step edges and step bunching occurred immediately. It was found that the average macrostep spacing increases in accordance with the domain sizes to a saturated value at a certain temperature. With an increase of the growth temperature, macrostep spacing was increased to cover hundreds of monatomic steps until the surface became a pure $(1\times 1)_{\text{HT}}$ reconstruction. However, as soon as the growth temperature was lowered down to 620°C , step debunching occurred immediately in a few minutes with remarkable step motion.

Studies concerning the behavior of atomic steps during the evolution of semiconductor surfaces, such as Si (Ref. 1) and GaAs (Refs. 2 and 3), is of great fundamental interest and technological importance. An understanding of the step bunching mechanisms is essential to modify the surfaces for the *in situ* fabrication of novel materials structures.^{2,4} Many origins have been proposed to give rise to step bunching caused by, for example, asymmetric incorporation of atoms from the upper and lower terraces into the atomic steps, known as the Schwoebel effect,⁵ relaxation of vicinal strained layers,⁶ phase-transition⁷ and impurity contamination.⁸ It is crucial to find the mechanisms as well as to evaluate and complement the present theories and explanations by experimental evidence, especially by direct microscopic observations. In recent years, the combination of electron microscopy, scanning tunneling microscopy (STM), and atomic force microscopy (AFM) with the vapor-phase-epitaxial systems has made it possible to observe *in situ* the growing or grown surfaces in atomic scale. Among them, only scanning reflection electron microscopy^{9,10} (SREM) and scanning electron microscopy^{7,11,12} (SEM) are practically applicable in the growth ambient, such as molecular-beam epitaxy (MBE), without interrupting the growth. Only SEM images in the secondary electron mode have been able to resolve monatomic steps and islands on the GaAs(001) surface.¹¹

We employed a microprobe reflection-high-energy electron diffraction (μ -RHEED)/SEM MBE system which is similar to Ref. 11 for the real-time and real-space investigation of the step behaviors on MBE GaAs(111)*B* surfaces. In the previous paper,¹³ we reported the real-time observation of transitions between $\sqrt{19}\times\sqrt{19}$ reconstruction and 1×1 high-temperature reconstruction, known as $(1\times 1)_{\text{HT}}$, on GaAs(111)*B* vicinal surfaces under annealing without intentional growth. This paper reports the real-time imaging of reconstruction transitions on the GaAs(111)*B* vicinal surfaces during MBE of GaAs. Step moving, step bunching, and

debunching behaviors related to the reconstruction transitions were studied, and the step bunching mechanism is discussed.

The μ -RHEED/SEM MBE system used for this study consists of a SEM (Hitachi S-800) and a specially designed MBE chamber with Knudsen cells.¹² The substrates are misoriented GaAs(111)*B* inclined 1° toward the $[\bar{1}1\bar{2}]$ direction, or the average monatomic step spacing on the surface is 18.7 nm . After cleaning and etching by $\text{NH}_4\text{OH}:\text{H}_2\text{O}_2:\text{H}_2\text{O}=4:1:20$ for 2 min, they were mounted onto the Mo block by indium and transferred into the growth chamber. During the observation, a 25-keV electron beam from a field emission gun is focused onto the sample surface by a glancing angle of 10° with the azimuth along the $[\bar{1}10]$ direction, and the secondary electron image of the surface is obtained on the screen in real time. The scanning time for taking a photograph is 80 s, so that the time-dependent step motion or reconstruction transition can be recorded. In order to enhance the resolution of atomic steps, a tilt compensation of 70° was applied so that the step height is amplified by a factor of 6. After a GaAs buffer layer was grown, surface reconstruction transitions and the transition-associated step behavior during MBE growth were studied by changing the growth temperature under a constant growth rate of 0.1 ML/s and an arsenic pressure of 2×10^{-6} torr. The equivalent As/Ga flux ratio is 10.

During the growth of the buffer layer at 620°C , the surface reconstruction is $\sqrt{19}\times\sqrt{19}$. Real-time observation showed that under a growth rate of 0.3 ML/s , there always appeared macrosteps of a few monatomic layers and the macrostep edges are rough. A typical photograph taken during the growth is shown in Fig. 1(a). Steps proceed down from the left to the right. The average macrostep size is about 3.5 monatomic steps. After the growth rate was reduced to 0.1 ML/s without growth interruption, step edges became straight and uniformly spaced in a few minutes, as shown in Fig. 1(b). The resolved average step size was reduced to be about 2 monatomic steps. Because it takes 80 sec for the

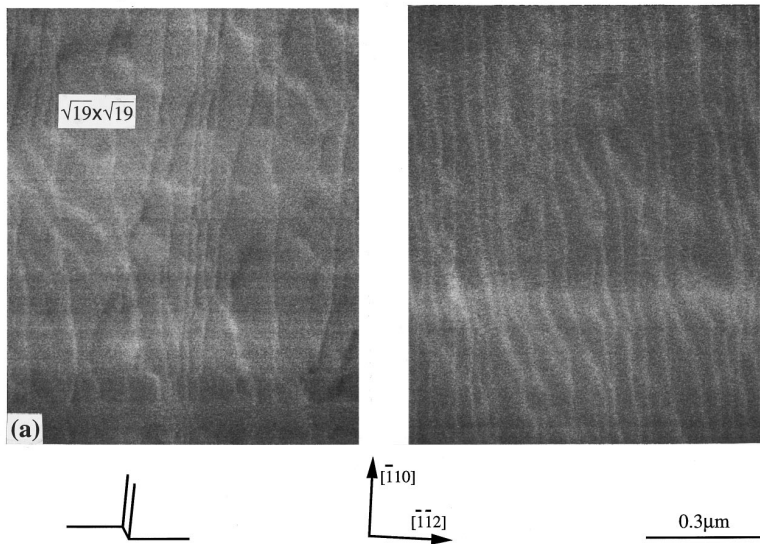


FIG. 1. Step structures during MBE of GaAs on the misoriented GaAs(111)*B* surface inclined 1° toward the $[\bar{1}\bar{1}2]$ direction under $\sqrt{19}\times\sqrt{19}$ reconstruction. The growth temperature is 620°C and the As pressure is 2×10^{-6} torr. (a) Growth rate of 0.3 ML/s. (b) Growth rate of 0.1 ML/s, the tilts of step edges from the $[\bar{1}10]$ direction are related to the step motion while taking the photograph.

electron scanning of one photograph, the tilt of the step edges from $[\bar{1}10]$ orientation is related to the step motion along the $[\bar{1}\bar{1}2]$ direction during the time delay for taking the photograph. The average velocity was estimated to be about 1.5 nm/s. This is very close to the theoretical prediction assuming step flow with uniformly spaced monatomic steps is preserved on the surface.

As the growth temperature was raised to 625°C while keeping other growth parameters constant, it was observed that bright domains appeared immediately from the step edges and step bunching occurred simultaneously. Figure 2(a) was taken after 5 min growth at 625°C . The $\sqrt{19}\times\sqrt{19}$ reconstructed dark domains were divided into stripes and those bright domains were confirmed to be under $(1\times 1)_{\text{HT}}$ reconstruction by μ -RHEED. The average macrostep size was increased to 3.5 monatomic steps. Some macrosteps with straight step edges along the $[\bar{1}10]$ direction were moving with negligible velocity, while those step edges with some tilts from the $[\bar{1}10]$ direction were probably moving quickly toward the $[\bar{1}\bar{1}2]$ direction during the time for taking the photograph. Since the contrast between $\sqrt{19}\times\sqrt{19}$ and $(1\times 1)_{\text{HT}}$ reconstructed domains differ greatly, monatomic steps moving on the terraces were not resolved. In 5 min after Fig. 2(a) was taken, the change in the average macrostep spacing was inconspicuous. Then the growth temperature was increased to 630°C . Figures 2(b), 2(c), and 2(d) were taken after the growth at 630°C for 1, 10, and 20 min, respectively. The average macrostep size was increased remarkably from 4 monatomic steps, to 10 and 12 monatomic steps, respectively. This means the macrostep spacing is saturated gradually if the temperature is kept constant. In Fig. 2(b), the $\sqrt{19}\times\sqrt{19}$ domains were first shrunk into round shapes on the terraces, and other terrace areas have been transformed into $(1\times 1)_{\text{HT}}$ reconstruction. Although the surface coverage of $\sqrt{19}\times\sqrt{19}$ domains should be mainly determined by thermodynamic factors, it increased slightly due to the increase of the terrace sizes during the continuous growth as we compared Fig. 2(c) with Fig. 2(d). By further increasing the growth temperature to 635°C , the $\sqrt{19}\times\sqrt{19}$ domains were completely removed, and a largely spaced macrostep morphology with abrupt and straight macrostep

edges was obtained, as shown in Fig. 3(a). The average macrostep size has been increased to about 50 monatomic steps and were stable during the following growth for about 10 min. The endings of macrosteps are easily observed as were indicated by arrows in Fig. 3(a). The appearance of the macrostep endings also indicates that monatomic steps are preserved on the macroterraces which are not resolvable in the above photographs.

The growth temperature was lowered down to 620°C . When it was passing 625°C , reconstruction transition from bright $(1\times 1)_{\text{HT}}$ to dark $\sqrt{19}\times\sqrt{19}$ occurred quickly as shown in Fig. 3(b), followed by remarkable step debunching since those heavily bunched macrosteps became unstable under $\sqrt{19}\times\sqrt{19}$ reconstruction. Figure 3(c) was taken after 5 min growth under the temperature of 620°C . The filled triangles indicate the splitting of three major macrosteps. The step debunching process also gave rise to fast step motion along the step down direction as the step edges were tilted away from the $[\bar{1}10]$ direction due to the time delay for recording the photograph. After a growth of 15 min, a uniformly stepped surface morphology with an average macrostep size of 3.5 monatomic steps was observed as shown in Fig. 3(d). Complete debunching of the macrosteps is expected by further growth.

As has been discussed in Ref. 14, when the crystal is grown at the reconstruction transition temperature, it is expected that immediately behind the fast moving steps the newly formed surface has not reconstructed, or has the phase which is more closer to the bulk crystal. Then, small reconstructed regions nucleate randomly on the newly formed terraces behind the moving steps. Because the nucleation and growth of the reconstructed regions are mainly thermodynamically controlled and are relatively slow, these reconstructed regions may have to be destroyed when the new layer is forming over them. It is reasonable to assume that growth on the reconstructed regions of the surface is more difficult than that on the unreconstructed areas. This probably makes the monatomic step motion slow down on the reconstructed regions.

The present real-time observation proved the above assumption that during the growth at the phase transition tem-

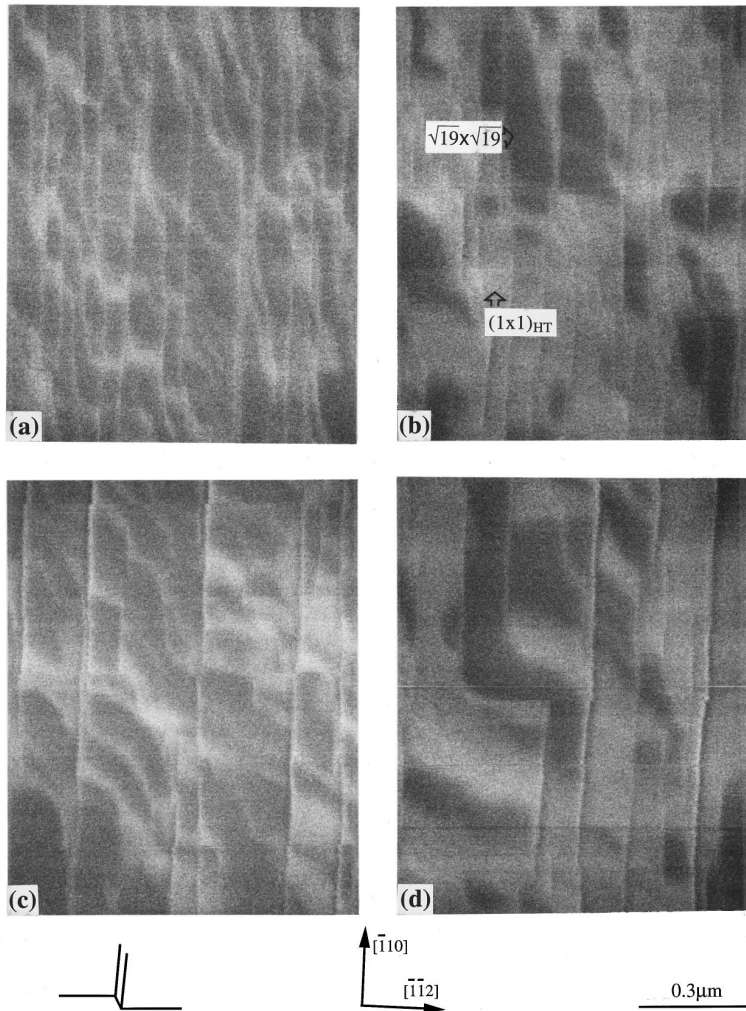


FIG. 2. SEM images of reconstruction transition from $\sqrt{19} \times \sqrt{19}$ to $(1 \times 1)_{HT}$ reconstruction and associated step bunching during MBE GaAs on the misoriented $(111)B$ surface inclined 1° toward the $[\bar{1}\bar{1}2]$ direction during raising the growth temperature. (a) After 5 min growth at 625°C , $(1 \times 1)_{HT}$ reconstructed bright domains were formed at the step edges and step bunching occurred simultaneously. Then (b) after 1 min, (c) after 10 min, and (d) after 20 min growth at 630°C , respectively.

perature, which is 625°C in this study, the newly formed step edges are of $(1 \times 1)_{HT}$ reconstruction, which is closer to the bulk phase. When the atomic step spacing is small enough, $\sqrt{19} \times \sqrt{19}$ reconstructed nucleation does not occur on such narrow terraces, so that $(1 \times 1)_{HT}$ reconstruction is formed where the step density is high. On the contrary, those terraces with wide step spacings are transformed into $\sqrt{19} \times \sqrt{19}$ reconstruction. Under this condition, the upper terrace side of a step is under the $(1 \times 1)_{HT}$ reconstruction while the lower one is under the $\sqrt{19} \times \sqrt{19}$ reconstruction during the step motion on the $\sqrt{19} \times \sqrt{19}$ reconstructed terraces. This kind of anisotropy gives rise to step bunching. Since monatomic steps do not block the development of the domains, the $\sqrt{19} \times \sqrt{19}$ domain sizes grow with the increase of the macrostep spacings. This positive feedback accelerates the step bunching before other kinetic processes take the major role. Concerning the fact that once the $(1 \times 1)_{HT}$ reconstructed domains appear on the $\sqrt{19} \times \sqrt{19}$ reconstructed GaAs(111) B vicinal surface, step bunching occurs either during the growth or during the annealing,¹³ it is concluded that this kind of step bunching behavior is somewhat similar to the impurity-induced step bunching as the $\sqrt{19} \times \sqrt{19}$ reconstructed domains behave as generalized impurities.

At a growth temperature within the reconstruction transition region between 625°C and 630°C in this study, it is found that the nucleation of the domains on the differently reconstructed surface is very slow. This is probably because

of insignificant driving force for the reconstruction transition in the coexisting condition. When $\sqrt{19} \times \sqrt{19}$ reconstruction becomes unstable and $(1 \times 1)_{HT}$ reconstructed domains develop from the step edges, step bunching occurs and the macrostep sizes increase until they are confined by other kinetic factors such as step-step interaction or the limited surface diffusion length.

On the contrary, if the temperature is decreased to have the transition from $(1 \times 1)_{HT}$ to $\sqrt{19} \times \sqrt{19}$ reconstruction during the growth, even the newly formed step edges are of or transformed into $\sqrt{19} \times \sqrt{19}$ reconstruction immediately. Under this growth condition, step bunches become unstable and are decomposed quickly during the growth. This also confirms that the step bunching process in the present study is caused by the presence of $(1 \times 1)_{HT}$ reconstructed domains. It also proves our previous study that by choosing a low growth rate and high As/Ga flux ratio under the $\sqrt{19} \times \sqrt{19}$ reconstruction, a smooth GaAs(111) B surface can be obtained.¹⁵ While selecting a low As/Ga flux ratio for the growth under the $\sqrt{19} \times \sqrt{19}$ reconstruction, another mechanism such as the Schwoebel effect⁵ may give rise to step bunching as has been discussed in Ref. 15 which does not work in the present study.

In summary, real-time imaging of reconstruction transitions during MBE on the GaAs(111) B surface was performed by secondary-electron SEM. Step moving, bunching, and debunching behaviors related to the reconstruction tran-

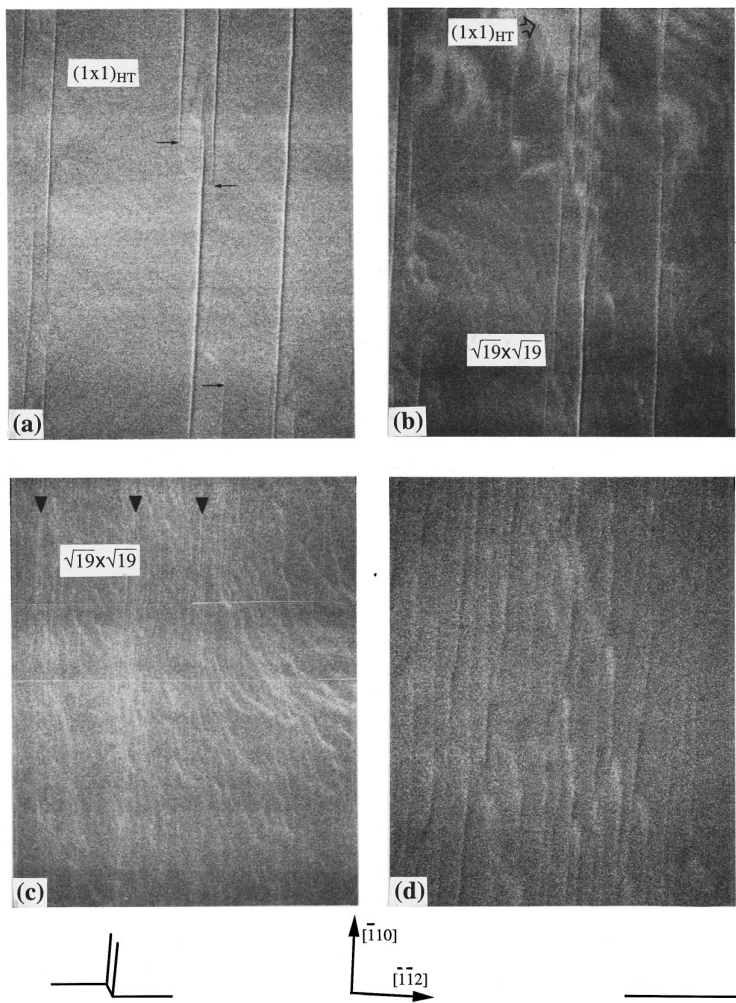


FIG. 3. SEM images of the step structures during MBE GaAs on the misoriented $(111)B$ surface inclined 1° toward the $[\bar{1}\bar{1}2]$ direction (a) when the surface was transformed into $(1 \times 1)_{HT}$ completely at 635°C . (b) By lowering the temperature to 620°C , reconstruction transition occurred at the top of the image when passing 625°C . Then (c) after 5 min, and (d) after 10 min growth at 620°C , respectively under $\sqrt{19} \times \sqrt{19}$ reconstruction. The scales for (a), (b), and (c) represent $1 \mu\text{m}$, while that for (d) represents $0.3 \mu\text{m}$.

sitions were studied. When the growth temperature of a $\sqrt{19} \times \sqrt{19}$ reconstructed surface is raised to the transition-point, $(1 \times 1)_{HT}$ reconstructed domains start to appear from the step edges and step bunching occurs simultaneously. With the increase of the growth temperature, macrostep sizes increase remarkably until the surface becomes pure $(1 \times 1)_{HT}$ reconstruction. This reconstruction transition associated step bunching is explained by the generalized impurity effect. As soon as the growth temperature is lowered to transform the surface back into $\sqrt{19} \times \sqrt{19}$ reconstruction,

step debunching occurs immediately with remarkable step motion.

We would like to thank Dr. X-Q. Shen, Dr. M. Tanaka, and Dr. Y. Homma for the valuable discussions. H.-W. Ren would like to thank the Japan Society for the Promotion of Science (JSPS) for financial support. This research was supported by Grants-in-Aid for Scientific Research on Priority Areas "Crystal Growth Mechanism in Atomic Scale" Nos. 03243102 and 04227101 from the Ministry of Education, Science and Culture, Japan.

*Present address: Masumoto Single Quantum Dot Project, ERATO, JST, Tsukuba Research Consortium, 5-9-9 Tokodai, Tsukubashi, 300-26, Japan.

¹A. V. Latyshev, A. L. Aseev, A. B. Krasilnikov, and S. I. Stenin, *Surf. Sci.* **213**, 157 (1989).

²J. Ishizaki, S. Goto, M. Kishida, T. Fukui, and H. Hasegawa, *Jpn. J. Appl. Phys.* **33**, 721 (1994).

³C. W. Snyder, J. Sudijono, C. H. Lam, M. D. Johnson, and B. G. Orr, *Phys. Rev. B* **50**, 18 194 (1994).

⁴M. Takeuchi, K. Shiba, H. K. Huang, K. Sato, K. Inoue, K. Maehashi, and H. Nakashima, *J. Cryst. Growth* **150**, 441 (1995).

⁵R. L. Schwoebel, *J. Appl. Phys.* **40**, 614 (1969).

⁶J. Tersoff, Y. H. Phang, Z. Y. Zhang, and M. G. Lagally, *Phys. Rev. Lett.* **75**, 2730 (1995).

⁷H. Yamaguchi, Y. Homma, and Y. Horikoshi, *Appl. Phys. Lett.* **66**, 1626 (1995).

⁸F. C. Frank, in *Growth and Perfection of Crystals*, edited by R. Doremus, B. Roberts, and D. Turnbull (Wiley, New York, 1958), p. 411.

⁹M. Ichikawa and T. Doi, *Appl. Phys. Lett.* **50**, 1141 (1987).

¹⁰T. Isu, A. Watanabe, M. Hata, and Y. Katayama, *Jpn. J. Appl. Phys.* **27**, L2259 (1988).

¹¹Y. Homma, J. Osaka, and N. Inoue, *Jpn. J. Appl. Phys.* **33**, L563 (1994).

¹²T. Suzuki and T. Nishinaga, *J. Cryst. Growth* **142**, 49 (1994).

¹³H.-W. Ren and T. Nishinaga, *Appl. Phys. Lett.* **69**, 565 (1996).

¹⁴D. Kandel and J. Weeks, *Phys. Rev. B* **49**, 5544 (1994).

¹⁵H.-W. Ren, X.-Q. Shen, and T. Nishinaga, *J. Cryst. Growth* (to be published).